Supplementary Information

Hollow porous prismatic graphitic carbon nitride with nitrogen vacancies and oxygen doping: a high-performance visible light-driven catalyst for nitrogen fixation

Ting Huang[a,b], Shugang Pan[a], Lingling Shi[a], Aiping Yu[b], Xin Wang[a,*] and Yongsheng Fu[a,*]

[a] Key Laboratory for Soft Chemistry and Functional Materials of Ministry of Education, Nanjing University of Science and Technology, Nanjing 210094, China

[b] Waterloo Institute for Nanotechnology, University of Waterloo, Waterloo, Ontario N2L3G1, Canada

* Corresponding authors

E-mail addresses: fuyongsheng0925@163.com, fuyongsheng@njust.edu.cn (Y. S. Fu), wangx@njust.edu.cn (X. Wang)

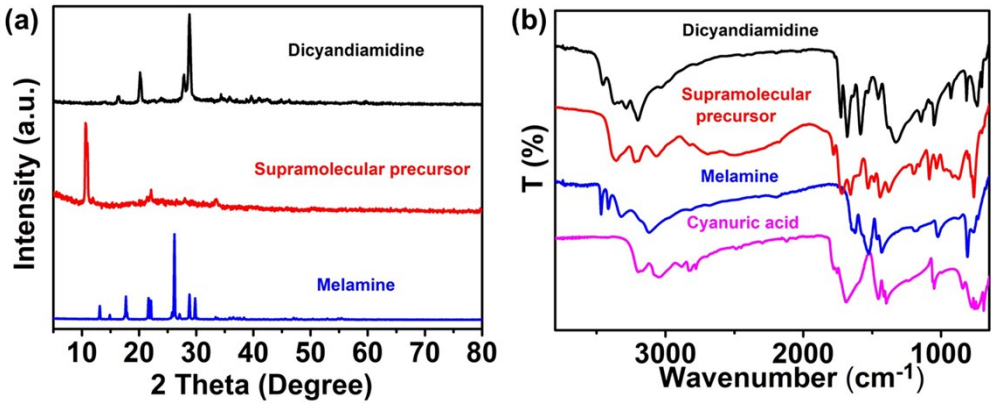

Fig. S1 (a) X-ray diffraction (XRD) of the dicyandiamidine, supramolecular precursor, melamine and cyanuric acid. (b) FT-IR spectra of the dicyandiamidine, melamine and supramolecular precursor.

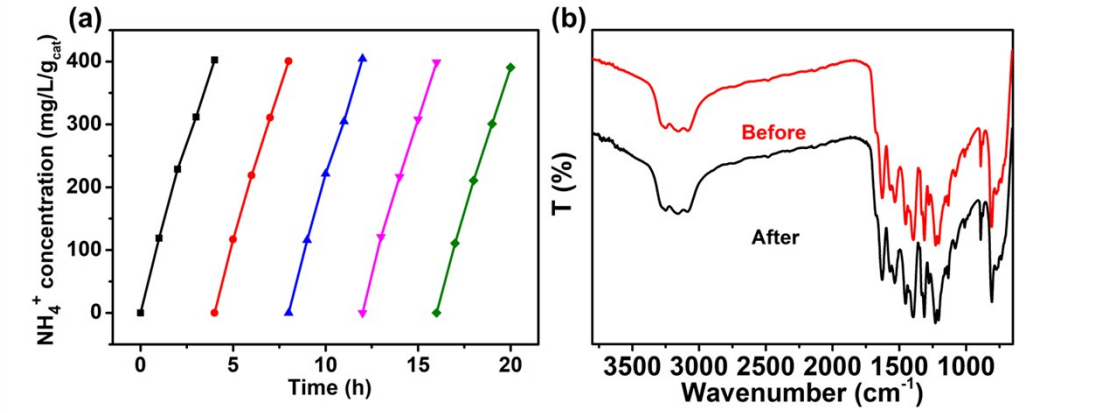

Fig. S2 (a) The cycling testing of the photocatalytic activity over 20 h for N*v*&O*d*-CN under the visible light irradiation ($\lambda > 420$ nm), (b) FI-IR spectra of N*v*&O*d*-CN before and after reaction.

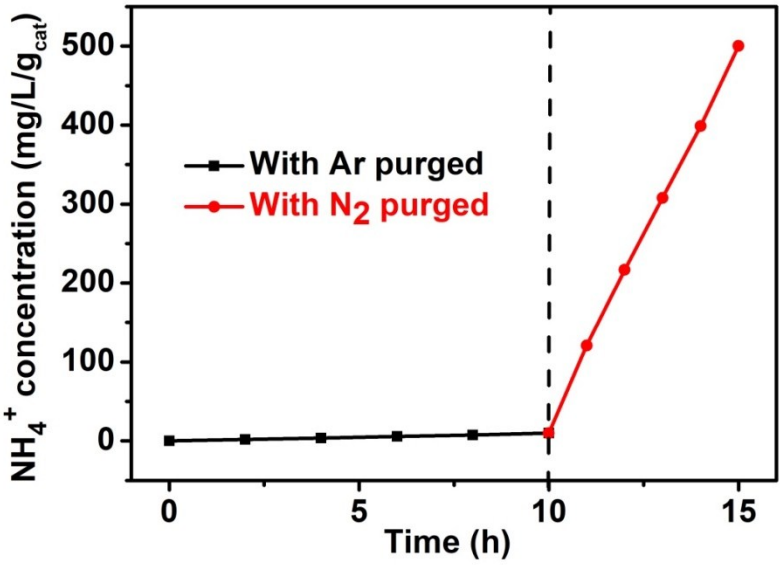

Fig. S3 Photocatalytic nitrogen fixation for N*v*&O*d*-CN under the visible light irradiation (λ > 420 nm) with Ar purged or N_2 purged.

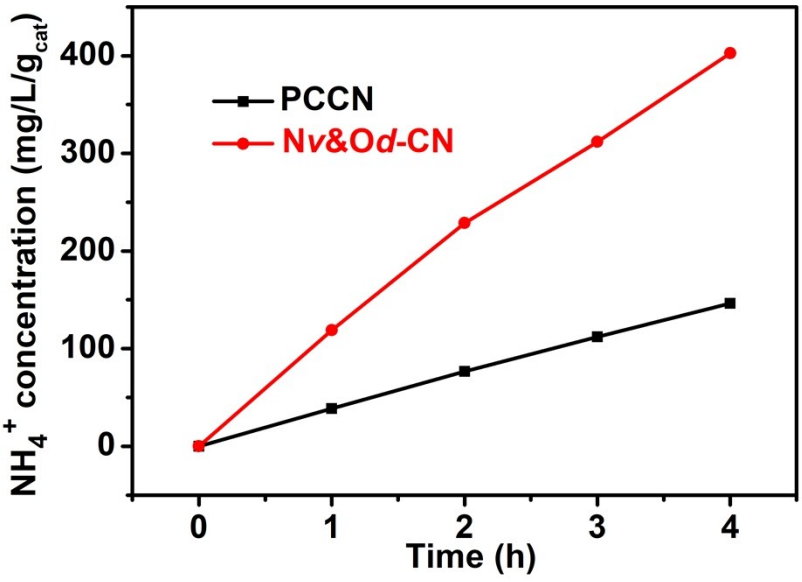

Fig. S4 Photocatalytic nitrogen fixation for PCCN and N*v*&O*d*-CN under the visible light irradiation (λ > 420 nm).

The porous crimped graphitic carbon nitride (PCCN) with a large specific surface area

(146.14 m^2 g^{-1}) was prepared based on our previous work (*Appl. Surf. Sci. 2019, 480: 888–895*) and was used as the contrast sample, which has neither nitrogen vacancies nor oxygen doping for the PCCN. The photocatalytic nitrogen fixation performances over the N*v*&O*d*-CN and PCCN have been carried out under visible-light irradiation at room temperature and the results are shown in Fig. S4. It is noteworthy that although both the PCCN and N*v*&O*d*-CN possess large specific surface area, the nitrogen fixation rate of PCCN is obviously lower than that of N*v*&O*d*-CN, indicating that the change of specific surface area is not a mainly factor for improving photocatalytic nitrogen fixation performance.

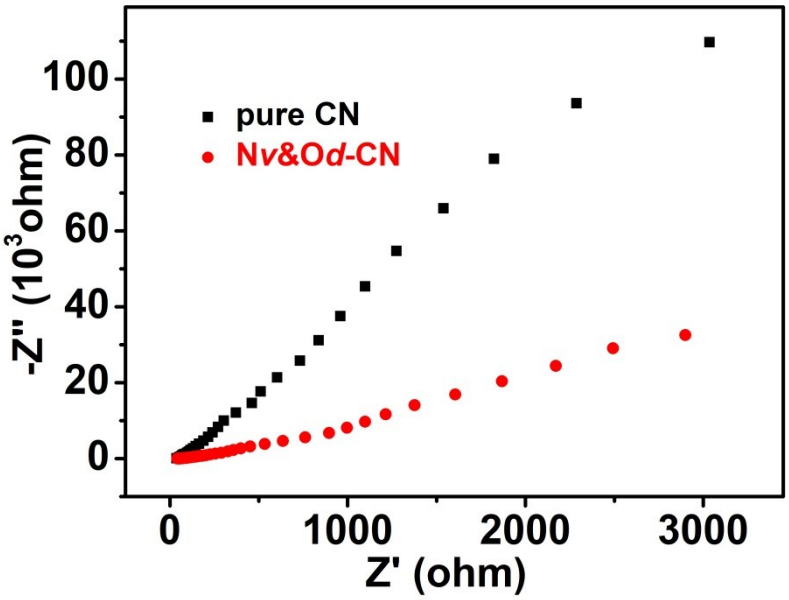

Fig. S5 EIS Nyquist plots of the pure CN and N*v*&O*d*-CN.

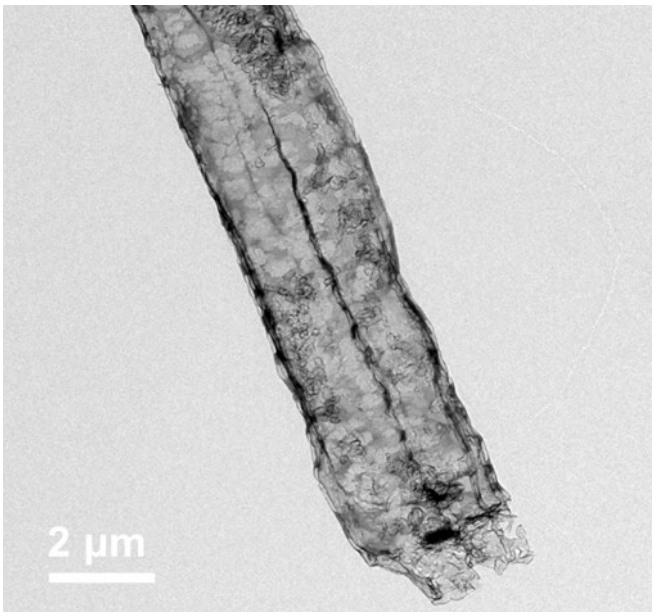

Fig. S6 TEM images of CN1.

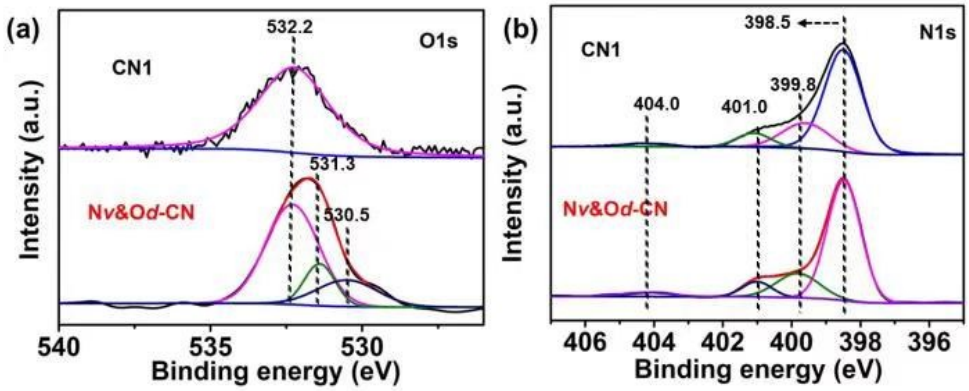

Fig. S7 (a) XPS high resolution O 1s and (b) N 1s spectra for CN1 and N*v*&O*d*-CN.

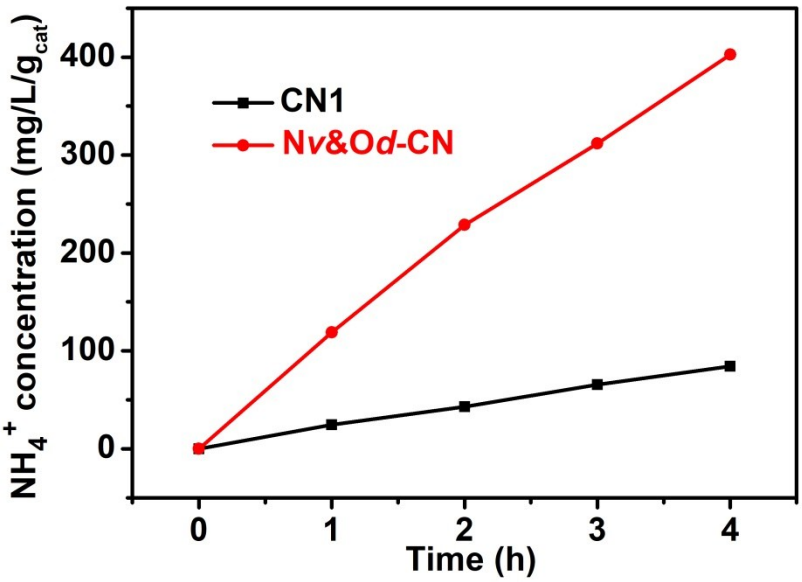

Fig. S8 Photocatalytic nitrogen fixation for CN1 and N*v*&O*d*-CN under the visible light irradiation (λ > 420 nm).

Table S1 Elemental analysis of the pure CN and N*v*&O*d*-CN.

Samples	N (wt.%)	C (wt.%)	H (wt.%)	O (wt.%)
Pure CN	55.31	42.18	2.37	0.17
N*v*&O*d*-CN	51.76	41.08	1.93	5.23

Table S2 The peak areas of N species of the pure CN and N*v*&O*d*-CN.

Samples	N_{2C} area	N_{3C} area	N_{NHx} area
Pure CN	35713	11702	3423
N*v*&O*d*-CN	33048	8553	3697

References

1 T. Huang, Y.S. Fu, Q. Peng, C.Y. Yu, J.W. Zhu, A.P. Yu and X. Wang, *Appl. Surf. Sci.,* 2019, **480,** 888–895.